EFFECTS OF IL-36Γ-MEDIATED P38 MAPK/ERK1/2 SIGNALING PATHWAY ON THE TISSUE REMODELING OF NASAL MUCOSA IN RATS WITH CHRONIC RHINOSINUSITIS

J. Zeng, X. J. Li, and X. S. Li*

Department of Otolaryngology Head and Neck Surgery, The Fourth Hospital of Changsha (Integrated Traditional Chinese and Western Medicine Hospital of Changsha, Changsha Hospital of Hunan Normal University), Changsha, 410006, Hunan, China.

*Corresponding author's Email: lxshengxl@yeah.net

ABSTRACT

This study was aimed to investigate the effect of interleukin-36γ (IL-36γ) on nasal mucosal tissue remodeling in rats with chronic rhinosinusitis (CRS) through mediation of the p38 mitogen-activated protein kinase (p38 MAPK)/extracellular signal-regulated kinase 1/2 (ERK1/2) signaling pathway. Sixty healthy male rats were equally and randomly rolled into control group (sham operation + saline), CRS group (ovalbumin + lipopolysaccharide-induced CRS model), IL-36γ group (CRS model + intraperitoneal injection of IL-36γ inhibitor), MAPK group (CRS model + intraperitoneal injection of p38 MAPK inhibitor), IL-36γ negative control group (CRS model + inhibitor buffer), and p38 negative control group (CRS model + dimethyl sulfoxide buffer). Nasal symptoms and signs of the rats were regularly observed and recorded. The concentrations of IL-36γ, IL-1β, and TNF-α in serum were detected by enzyme-linked immunosorbent assay (ELISA). Nasal septum mucosal tissues were stained with hematoxylin and eosin (H&E) to observe histological structures, and eosinophils were manually counted using five randomly selected high-power fields per section. Alcian blue periodic acid schiff (AB-PAS) staining was performed to detect the number of goblet cells. Masson's trichrome staining determined the percentage area of collagen components. mRNA expression of three cytokines in rat nasal mucosa was detected by RT-qPCR. Western blotting detected expression changes of IL-36γ, key proteins of the MAPK pathway, and matrix metalloproteinase-9 (MMP-9) in nasal mucosa tissue. The nasal symptom scores were markedly increased in the CRS, IL-36γ, and MAPK groups versus controls (P<0.05). IL-36γ and MAPK groups exhibited a prominent reduction in nasal symptom scores, along with decreased eosinophil infiltration, goblet cell numbers, and collagen fiber deposition in nasal mucosa versus CRS group. IL-36γ, TNF-α, and IL-6 in both serum and nasal mucosa were reduced, and protein expression of IL-36γ, p-p38, p-ERK, and MMP-9 was substantially lower (P<0.05). The MAPK group demonstrated further reductions in serum and nasal mucosal levels of IL-1β, as well as in p-p38 and MMP-9 protein expression, versus the other treatment groups (P<0.05). Insignificant differences existed in all indicators among the IL-36γ negative control and the p38 negative control and the CRS groups (P>0.05).

Conclusion: IL-36γ-mediated p38 MAPK/ERK1/2 signaling affects tissue remodeling of nasal mucosal in rats with CRS by regulating MMP-9 expression, showcasing a critical therapeutic target in CRS progression. Targeting this signal pathway may provide a new therapeutic strategy for improving nasal mucosa integrity and relieving inflammatory symptoms in CRS.

Keywords: chronic rhinosinusitis; nasal mucosa; tissue remodeling; IL-36γ; p38 MAPK/ERK1/2 pathway

https://doi.org/10.36899/JAPS.2026.4.0078 Published first online May 01, 2026

INTRODUCTION

Chronic rhinosinusitis (CRS) is one form of rhinosinusitis (Sedaghat *et al.,* 2022). Its pathological features include nasal mucosal epithelial damage, goblet cell hyperplasia, and increased vascular permeability (Vlaminck *et al.,* 2021). Tissue remodeling is the key mechanism of chronic and severe CRS (Kucuksezer *et al.,* 2018), which involves mucosal epithelial injury and extracellular matrix (ECM) deposition. Imbalance between MMPs and tissue inhibitors (TIMPs) acts crucially (Enache *et al.,* 2020; Huang *et al.,* 2024). Despite attempts to intervene with antibiotics, corticosteroids, and surgery, CRS still faces the issue of recurrence or therapy resistance (Brzost *et al.,* 2022). Systematic study on the molecular mechanism of inflammatory disorder of rhinosinusitis helps promoting individualized therapy strategy.

IL-36γ promotes Th17 cell differentiation and neutrophil recruitment by activating NF-κB and MAPK pathways, then aggravating local inflammatory response (Qiao *et al.,* 2023). More and more evidences showed that IL-36γ expression level is enhanced in Th17-mediated diseases, including psoriasis and asthma (Chen *et al.,* 2021). Study foud that IL-36γ exhibited obvious expression level in nasal mucosa affected by rhinosinusitis (Qiao *et al.,* 2023). Therefore, IL-36γ may act in chronic airway inflammation. Nevertheless, although the existing research showed that IL-36γ expression level in CRS is increased, the specific regulatory mechanism is still unclear. Its influence on nasal mucosa structure and function and its potential feedback loop with neutrophils have not been clarified. P38 and ERK1/2 belong to two parallel branches of MAPK family, activated by different upstream kinases and jointly regulate cell biological processes, including stress response, proliferation, differentiation, and fibrosis (Emelyanova *et al.,* 2025). MMP-9 is involved in collagen degradation and tissue remodeling in CRS. P38 MAPK may play a dual role under the pathological background. For example, in the glioblastoma model, p38 MAPK may promote tumor progression by enhancing the expression of inflammatory genes (Kim *et al.,* 2025). This pathway shows anti-inflammatory potential in diseases like rheumatoid arthritis (Chen *et al.,* 2023). However, its specific function in CRS model and its regulatory effect on mucosal tissue remodeling remain unclear. Therefore, exploring how IL-36γ-p38 MAPK/ERK1/2 axis may affect CRS will help to clarify the molecular mechanism of disease progression and develop targeted treatment strategies.

In short, the role and molecular mechanism of p38 MAPK/ERK1/2 signaling mediated by IL-36γ in CRS nasal mucosa remodeling is still unclear. Therefore, this study aimed to investigate the effects of the IL-36γ-mediated p38 MAPK/ERK1/2 signaling pathway on nasal mucosal tissue remodeling in rats with CRS, elucidate its molecular mechanisms, and provide a theoretical basis for research on the pathogenesis of CRS and the development of targeted therapeutic strategies.

MATERIALS AND METHODS

Experimental animal grouping: Sixty healthy male SD rats (6–8 weeks, 137–183 g, with an average weight of 160.25 ± 20.36 g) were obtained from Chengdu Dashuo Experimental Animal Center, China. Animal housing environment was controlled, with temperature at 25 ± 1°C, relative humidity at 55 ± 2%, and standardized lighting conditions. All the experiments and procedures adhered to guidelines and were approved by the Ethics Committee of The Fourth Hospital of Changsha.

After two weeks of acclimatization, rats were randomly assigned into control, CRS, IL-36γ, MAPK, IL-36γ negative control, and p38 negative control groups (n=10/group). In the behavioral and histological assessment, the assessor knew nothing about group assignment to minimize subjective bias. The sample size of each group was determined according to the preliminary experimental results and the experience of using similar models in our laboratory, which ensures the stability and statistical reliability of the results in repeated experiments.

Control group: Sham surgery (exposing the nasal cavity without ovalbumin or inflammation-induced anesthesia) was performed, and then saline was injected intraperitoneally.

CRS group: CRS model was induced by intraperitoneal injection of ovalbumin combined with lipopolysaccharide to induce inflammation.

IL-36γ group: After CRS model establishment, rats received intraperitoneal injection of IL-36γ inhibitor.

IL-36γ negative control group: Following the establishment of the CRS model, an equivalent volume of saline supplemented with BK-KT10885 formulation buffer (devoid of antibodies) was administered via intraperitoneal injection to exclude non-specific effects.

MAPK group: After CRS model establishment, rats received intraperitoneal injection of p38 MAPK inhibitor.

p38 negative control group: After the CRS model was established, an equivalent volume of the SB203580 formulation solvent (dimethyl sulfoxide buffer, without inhibitor) was administered via intraperitoneal injection to exclude solvent and non-specific effects.

CRS model establishment: After two weeks of acclimatization, a CRS model was established in rats according to a previously described method (Kim *et al.,* 2016). Sensitization phase: A 1 mL suspension containing 0.3 mg ovalbumin (Sigma, USA) and 30 mg aluminum hydroxide (Sigma, USA) was administered via intraperitoneal injection every other day, totalling seven times. Two weeks after the last injection, local challenge was initiated: intranasal instillation of 5% ovalbumin solution (50 μL per nostril) was performed, accompanied by daily 1% ovalbumin aerosol inhalation (ultrasonic nebulization, 5 min) for 10 consecutive days. Following the challenge period, intranasal instillation of 5% ovalbumin (25 μL per nostril) was continued every other day. Additionally, Staphylococcus aureus enterotoxin B (SEB, 5 ng per rat, Sigma, USA) was administered intranasally once weekly for six weeks.

Intervention methods: After the CRS model was established, the IL-36γ group received intraperitoneal injection of IL-36γ neutralizing antibody (BK-KT10885, Boke Technology Co., Ltd., China) at 10 mg/kg, every 3 d, for 14 d. The IL-36γ

negative control group received an intraperitoneal buffer injection (equivalent volume, without antibody), following the same administration regimen as the IL-36γ group. The MAPK group received intraperitoneal injection of p38 MAPK inhibitor SB203580 (APExBIO Technology Co., USA) at 3 mg/kg, every 3 d, for 14 d. The p38 negative control group received an intraperitoneal dimethyl sulfoxide injection (equivalent volume, without inhibitor), following the same administration regimen as the MAPK group. The CRS group received no drug intervention on the CRS model. The Control group received only saline injection and no drug intervention.

Behavioral assessment: During the experiment, the nasal symptoms and signs were regularly observed and recorded. These included: Nasal itching: Observing whether rats frequently scratched their noses to determine if they felt nasal itching. Rhinorrhea: Observing the amount and state of nasal secretions to assess secretion quantity and quality. Sneezing: Recording the frequency of sneezing within a unit of time, specifically the number of sneezes in 30 min. Symptom severity was assessed using the rhinosinusitis symptom scoring criteria (Tu *et al.*, 2020) (Table 1).

Table 1 Rhinosinusitis symptom scoring criteria

Symptom	Mild (1 point)	Moderate (2 points)	Severe (3 points)
Nasal scratching frequency	1–4 times/30 min	5–9 times/30 min	≥10 times/30 min
Rhinorrhea	Mild secretion	Secretions flowing to the nostrils	Secretions adhering around the nose
Sneezing frequency	1–4 times/30 min	5–9 times/30 min	≥10 times/30 min
Nasal inflammation	Mild congestion	Redness and swelling	Redness, swelling, and bleeding

Enzyme-linked immunosorbent assay (ELISA): Blood was collected from the orbital sinus prior to euthanasia. After being left at 25°C for 30 min, the samples were centrifuged at 3,000 g for 15 min (4 °C), and in the generated serum, IL-36γ, IL-1β, and TNF-α were measured using ELISA kits (Shanghai Meilian Biotechnology Co., Ltd., China) strictly following preparation of standard gradients, sample and reagent loading, incubation, washing, color development, and reaction termination. Absorbance was finally measured at 450 nm via reader (F50, Tecan, Switzerland), and the concentrations of each indicator were calculated.

Histological assessment: On the day following the completion of drug interventions, rats were euthanized via cardiac exsanguination under isoflurane inhalation anesthesia (4%–5%, oxygen flow rate 1–2 L/min). The nasal dorsum was rapidly incised to extract nasal mucosal tissue, which was fixed in 4% paraformaldehyde for 24h. After dehydration through a graded alcohol series, xylene clearing, and paraffin embedding, sections were cut at a thickness of 4–5 μm using a microtome (RM2016, Leica, Germany) and baked at 60°C for 2 h. Histological examinations included hematoxylin and eosin (H&E) staining to observe the structure of the nasal septum mucosa and count eosinophils, alcian blue periodic acid schiff (AB-PAS) staining to quantify goblet cells and assess changes in secretory function, and Masson's trichrome staining to evaluate collagen fiber content in the nasal septum and basement membrane, with the area percentage calculated.

RT-qPCR: The mucosal tissues were removed and quickly washed to remove blood and other impurities. A total of 100 mg of the minced tissue was weighed and RNA was extracted based on the guidance of the Trizol reagent kit (YB73070, Shanghai Yubo Biotechnology Co., Ltd., China). An appropriate amount of Trizol reagent was applied, and the tissue was thoroughly lysed adopting a homogenizer on ice to ensure complete release of RNA. A Qubit fluorometer (Thermo Fisher, USA) adopted for measurement, and the integrity of RNA was checked. Reverse transcription was performed to synthesize cDNA from isolated RNA adopting the Maxima First Strand cDNA Synthesis Kit with dsDNase (EP0751, Thermo Fisher, USA). The reverse transcription system was 20 μL: 1 μg RNA, 2 μL 10 mmol/L dNTP, 4 μL 5× Buffer, 1 μL OligodT, and 0.5 μL reverse transcriptase. Reverse transcription program was 42°C for 50 min and 75°C for 10 min. 1 μL of the reverse transcription product was adopted as template, and RT-qPCR amplification was carried out adopting the QK Platinum SYBR Green Master Mix kit (A57155, Thermo Fisher, USA) by the SYBR method in a QuantStudio3 QS5 PCR instrument (Thermo Fisher, USA). Reaction conditions: initial denaturation at 95°C for 2 min; followed by 30 cycles of denaturation at 95°C for 15 s, annealing at 55°C for 34 s; and a final extension at 72°C for 5 min. GAPDH served as the reference gene to analyze the inflammatory factors in the nasal mucosa of rats with rhinosinusitis. Each reaction was performed in triplicate with an annealing temperature of 60°C, annealing time of 30 s, and 30 cycles. Gene relative expression was computed adopting $2^{-\Delta\Delta ct}$ approach. The sequences of the amplification primers for IL-36γ, IL-1β, TNF-α, and GAPDH are listed in Table 2, synthesized by Sangon Biotech Co., Ltd. (Shanghai, China).

Table 2. Primer for RT-qPCR amplification

Gene	Forward primer	Reverse primer
IL-36γ	5'-TACCACTCTGATTGTGGACTGC-3'	5'-CCCCTTCTCTGATTCGTTTGGA-3'
IL-1β	5'-TGGACCTTCCAGGATGAGGAC-3'	5'-GTTCATCTCGGAGCCTGTAGTG-3'
TNF-α	5'-CACACCCTGACAAGCTGACTGC-3'	5'-GACCGACTCAGCGCTGAGAT-3'
GAPDH	5'-AGTTCAACGGCACAGTCAAG-3'	5'-CAGCCTTCTCCATGGTGGTG-3'

Western blotting: The expression changes of IL-36γ, key proteins of MAPK pathway, and MMP-9 in nasal mucosa tissue were detected by Western blotting. All experiments were performed in triplicate to ensure reproducibility. A total of 100 mg of nasal mucosa tissue was weighed and placed into a homogenizer, minced as much as possible, and 1 mL of pre-prepared lysis buffer (RIPA protein lysis buffer: protease inhibitor PMSF=1:100) was applied for grinding. Mixture was placed on ice for 30 min, and centrifugation was carried out at 12,000 g (4°C, 20 min) to collect upper liquid. The protein concentration was measured. The proteins were denatured by boiling in water for 10 min. Proteins were separated by SDS-PAGE (10% separating gel, 5% stacking gel) and transferred to a polyvinylidene fluoride membrane adopting the wet transfer method at a constant current of 250 mA for 60-90 min. 5% skim milk was applied for blocking (1 h), incubation with diluted rabbit anti-rat IL-36γ (1:1000), p-p38 (1:1000), p-ERK (1:1000), p38 (1:2000), ERK (1:2000), MMP-9 (1:1000), and β-actin antibodies (1:5000) (Abcam, UK) overnight at 4°C. Membrane was thoroughly subjected to three rinses with TBST for 10 min each, incubation with HRP-conjugated secondary antibody (1:10000) (Shanghai Ruibosai Biotechnology Co., Ltd., China) at 25℃ for 2 h. The membrane was thoroughly rinsed thrice with TBST for 10 min each, and then the chemiluminescent substrate was applied. Protein bands were visualized using the GIS2009 imaging system (Tanon, China) and analyzed for grayscale intensity with *ImageJ* (National Institutes of Health, USA). Target protein levels were calculated by normalization to β-actin, presented as the mean±standard deviation (SD) from three independent experiments.

Statistical processing: *SPSS 19.0* was employed. Measurement data were represented as mean ± SD ($\bar{x} \pm s$). For measurement data meeting the normal distribution and homogeneity of variance, one-way ANOVA and Tukey's HSD test were adopted. For measurement data not meeting the homogeneity of variance, non-parametric tests were adopted. Categorical data were represented as percentages (%) and analyzed adopting χ^2 test. $P<0.05$ was statistically meaningful.

RESULTS

Signs and symptoms score analysis: Rat behavioral and nasal symptom scores are shown in Figure 1. The rhinorrhea, nasal scratching, and total symptom scores were increased in the CRS group (95% CI 7.32–8.32), IL-36γ negative control group (95% CI 7.19–8.11), and p38 negative control group (95% CI 7.22–8.20) versus controls ($P<0.001$). All scores were markedly reduced in the IL-36γ group (95% CI 3.68–4.16, $P<0.001$) and the MAPK group (95% CI 3.53–4.13, $P<0.001$) versus CRS group. The scores of the IL-36γ negative control group and the p38 negative control group were similar to CRS group, with insignificant improvement observed ($P>0.05$).

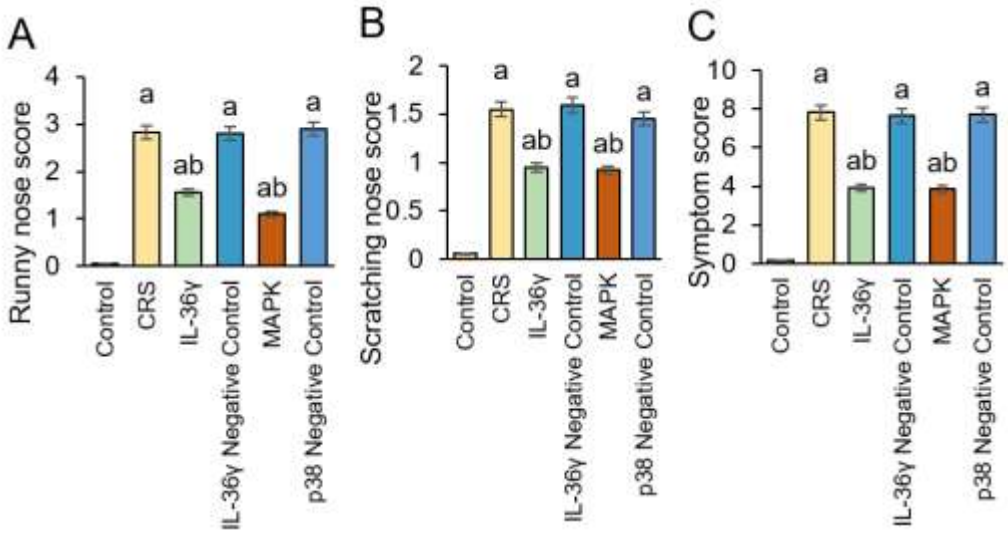

Figure 1 Contrast of behavioral and symptom scores. A: Rhinorrhea score; B: Nasal rubbing score; C: Symptom score. [a] vs. Controls, [b] vs. CRS group, *P*<0.05. The data were expressed as mean ± SD (n=10). Statistical comparisons were performed using ANOVA and Tukey's HSD tests.

Histological results: Histological analysis (Figure 2) revealed structural disorganization of the nasal mucosa in the CRS group, with eosinophil count (95% CI 18.82–26.90), goblet cell number (95% CI 18.04–21.26), and collagen fiber content (95% CI 18.04–21.26) markedly surpassing those in controls ($P<0.05$). These indicators were markedly reduced in the IL-36γ and MAPK groups versus the CRS group (eosinophils: 95% CI 12.02–19.14; goblet cells: 95% CI 11.17–13.53; collagen fibers: 95% CI 11.17–13.53) ($P<0.05$). The IL-36γ negative control group and p38 negative control group showed values similar to those of the CRS group, with negligible improvement (eosinophils: 95% CI 18.22–26.54; goblet cells: 95% CI 17.52–21.13; collagen fibers: 95% CI 17.55–21.06, $P>0.05$).

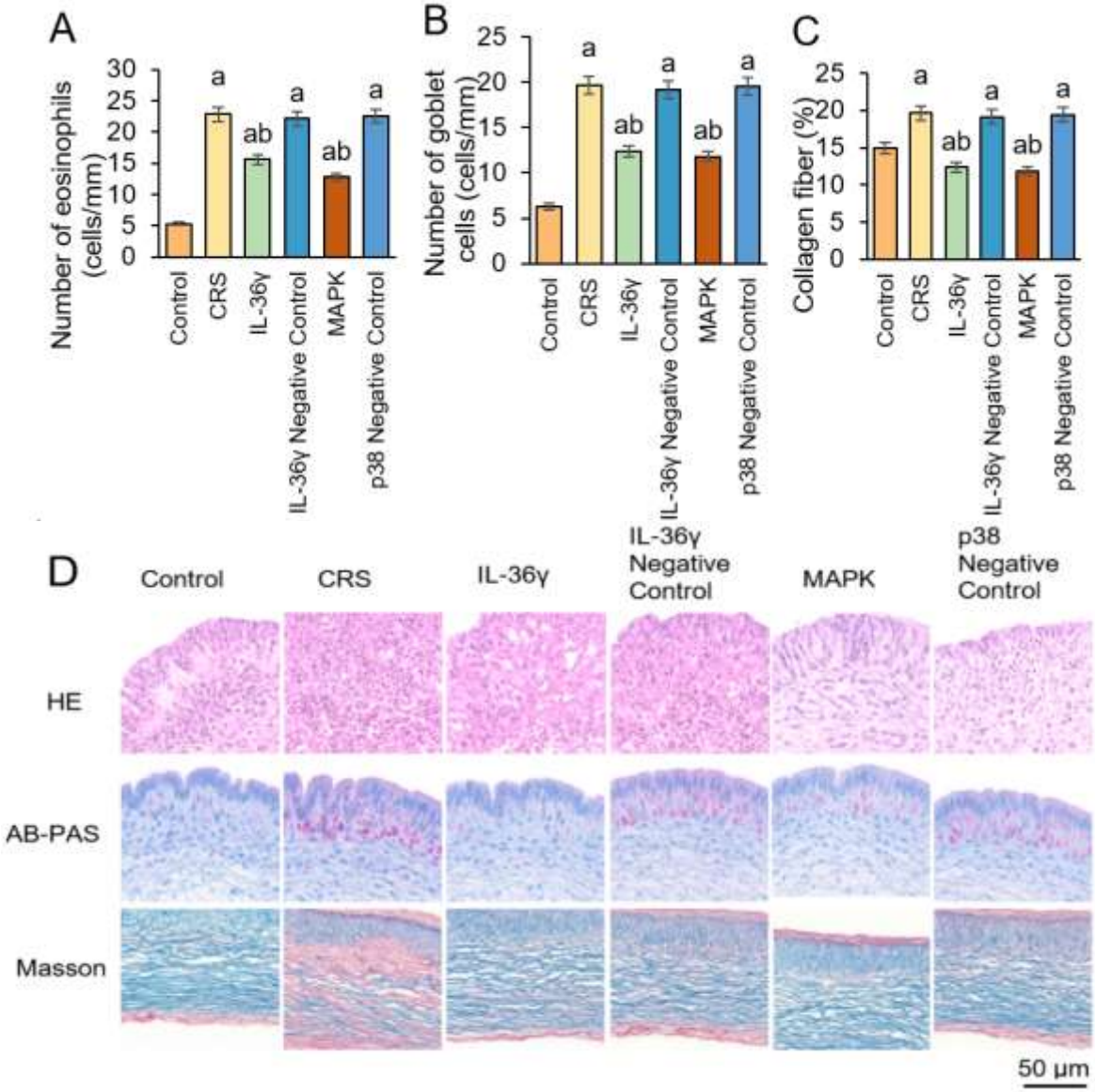

Figure 2 Histological results. A: Eosinophil count; B: goblet cells count; C: Collagen fiber content; D: images of H&E, AB-PAS, and Masson's trichrome staining. [a] vs. Controls, [b] vs. CRS group, *P*<0.05; Data were expressed as mean±SD (n=10). Statistical comparisons were performed adopting ANOVA and Tukey's HSD tests.

ELISA results analysis: CRS group exhibited markedly elevated serum IL-36γ, TNF-α, IL-6, and IL-1β (95% CI 250.1–275.6; 95% CI 25.8–31.6; 95% CI 60.4–71.2; 95% CI 72.3–85.6; $P<0.001$) versus controls. Relative to CRS group, IL-36γ

group showed marked reductions in IL-36γ, TNF-α, and IL-6 (95% CI 145.1–166.5; 95% CI 16.3–20.9; 95% CI 36.0–40.8; $P<0.05$), while IL-1β was slightly increased (80.02, 95% CI 75.1–84.9; $P>0.05$). The MAPK group demonstrated prominent decreases in IL-6, TNF-α, and IL-1β (95% CI 35.2–39.9; 95% CI 15.9–20.0; 95% CI 21.1–26.4; $P<0.05$). Serum inflammatory cytokine levels in the IL-36γ negative control group and the p38 negative control group were comparable to those in the CRS group ($P>0.05$), with slight improvement (Figure 3).

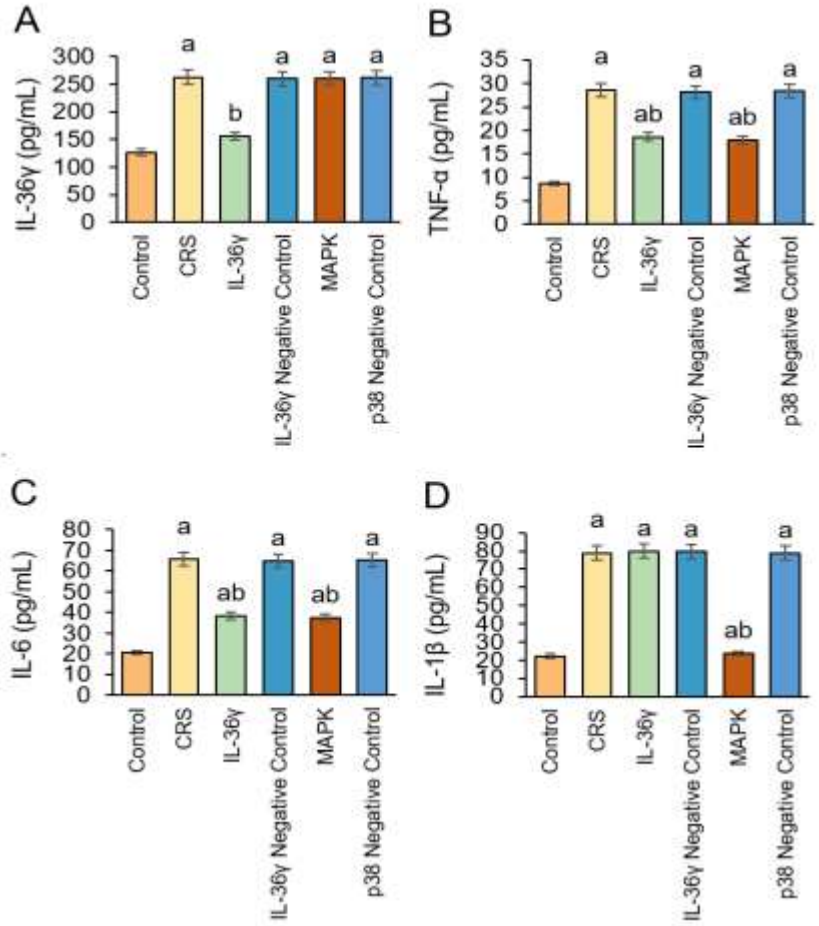

Figure 3 Contrast of serum inflammatory cytokine levels. A: IL-36γ; B: TNF-α; C: IL-6; D: IL-1β. [a] vs. Controls, [b] vs. CRS group, $P<0.05$; Data were denoted as mean±SD (n=10). Statistical comparisons were performed employing ANOVA and Tukey's HSD tests.

RT-qPCR results analysis: Relative to controls, CRS group exhibited elevated mRNA levels of IL-36γ, TNF-α, IL-6, and IL-1β in nasal mucosal tissues (95% CI: 3.01–3.47; 95% CI: 4.20–4.90; 95% CI: 3.38–3.92; 95% CI: 2.92–3.38; $P<0.05$). Relative to CRS group, the IL-36γ group demonstrated marked reductions in IL-36γ, TNF-α, and IL-6 mRNA (95% CI: 2.01–2.37; 95% CI: 2.01–2.37; 95% CI: 2.57–2.93; $P<0.05$), while the MAPK group demonstrated significant decreases in IL-6, TNF-α, and IL-1β mRNA (95% CI: 2.64–3.02; 95% CI: 1.98–2.34; 95% CI: 1.18–1.52; $P<0.05$). mRNA levels of all targets in the IL-36γ negative control group and the p38 negative control group were comparable to CRS group ($P>0.05$), but not significantly improved (Figure 4).

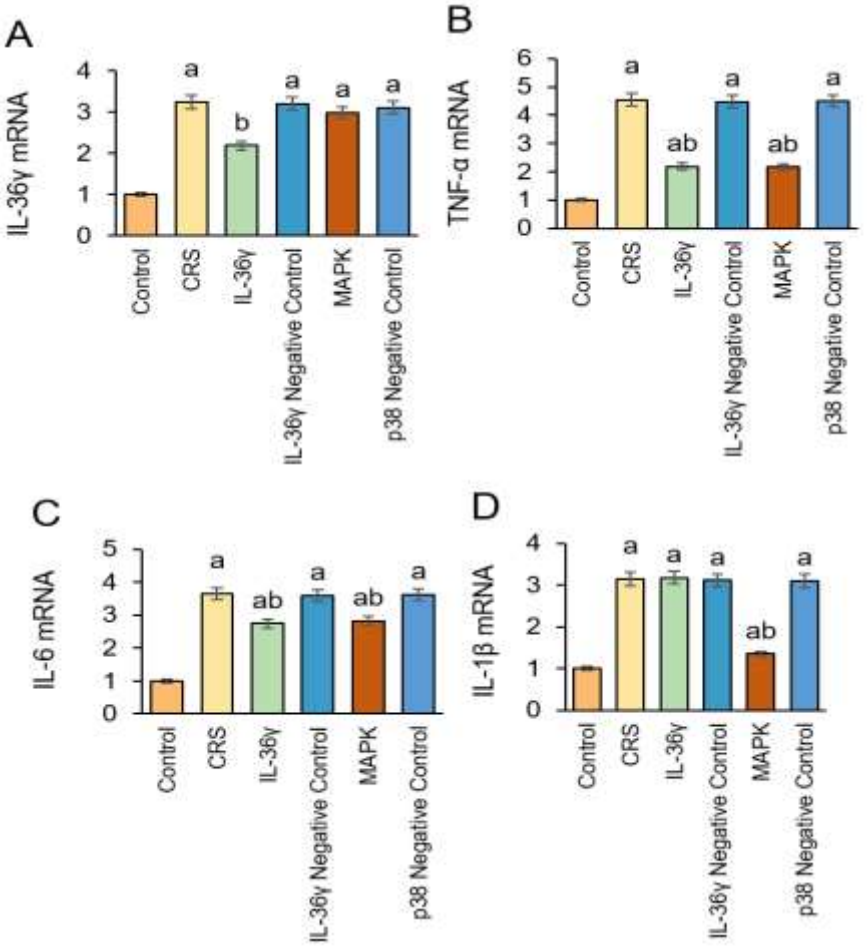

Figure 4 Contrast of inflammatory cytokine levels in nasal mucosa tissue. A: IL-36γ; B: TNF-α; C: IL-6; D: IL-1β. [a] vs. Controls, [b] vs. CRS group, *P*<0.05; Data were indicated as mean±SD (n=10). Statistical comparisons were performed via ANOVA and Tukey's HSD tests.

Western blotting results analysis: CRS group exhibited greatly elevated protein levels of IL-36γ, p-p38, p-ERK, and MMP-9 (95% CI: 2.90–3.58; 1.80–2.30; 1.95–2.45; 3.10–3.80; $P<0.05$) versus controls. Relative to CRS group, IL-36γ group had marked reductions in the relative expression of these proteins (95% CI: 2.00–2.38; 1.30–1.70; 1.50–2.00; 2.50–3.00; $P<0.05$), while the MAPK group demonstrated drastic decreases in p-p38 and MMP-9 (95% CI: 1.10–1.50; 2.40–2.80; $P<0.05$). Protein expression in the IL-36γ negative control group and the p38 negative control group was comparable to CRS group ($P>0.05$). The total p38 and total ERK protein levels exhibited insignificant differences across all groups ($P>0.05$) (Figure 5).

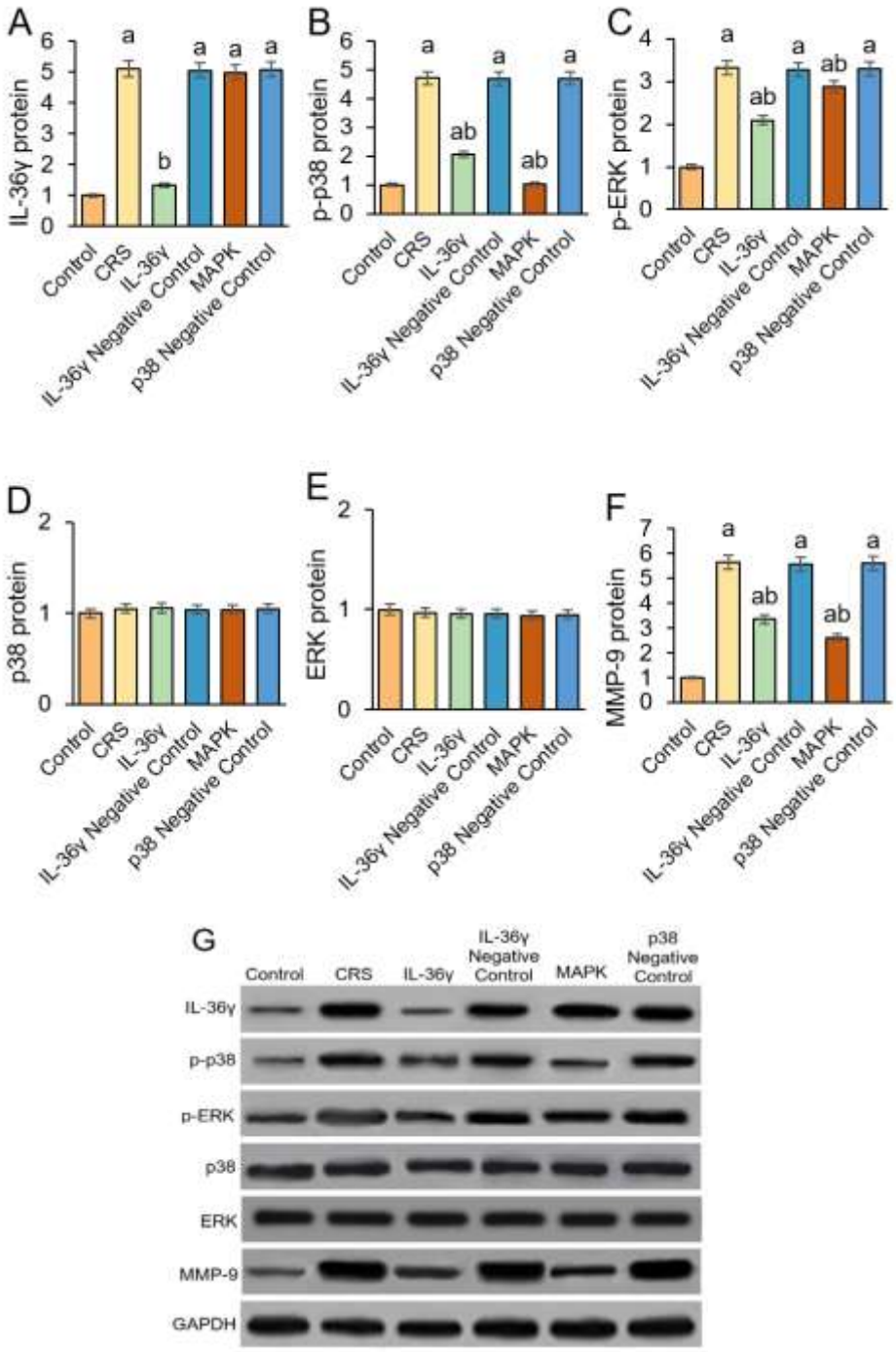

Figure 5 Contrast of protein expression in nasal mucosa tissue. A: IL-36γ; B: p-p38; C: p-ERK; D: p38; E: ERK; F: MMP-9; G: Western blotting image. [a] vs. Controls, [b] vs. CRS group, *P*<0.05; Data were denoted as mean±SD (n=10). Statistical comparisons were performed utilizing ANOVA and Tukey's HSD tests.

DISCUSSION

This study investigated the effects of the IL-36γ-mediated p38 MAPK/ERK1/2 signaling pathway on nasal mucosal tissue remodeling by establishing a CRS rat model. It was found that inhibiting IL-36γ and p38 signaling can significantly improve nasal mucosal tissue damage and reduce inflammatory response, indicating that this pathway plays a key role in tissue remodeling in rats with rhinosinusitis.

IL-36α, β, γ, and IL-36Ra are produced by immune, nerve, keratinocyte, and bronchial epithelial cells (Garlanda *et al.,* 2013; Gabay *et al.,* 2015; Wißbrock *et al.,* 2019). IL-36γ can activate NF-κB pathway, triggering production of IL-6 and IL-8 (Cloitre *et al.,* 2019). IL-36 cytokines can induce keratinocytes to produce neutrophil chemokines, promoting infiltration of neutrophils in psoriasis (Johnston *et al.,* 2017). Our study observed a similar outcome that the expression of IL-36γ increased substantially in CRS model, and its inhibition reduced inflammatory cell infiltration and cytokine production. It was suggested that IL-36γ can help promoting neutrophil inflammation in various inflammatory environments in a conservative manner. As confirmed, IL-36γ activation may act on neutrophils, exacerbating neutrophilic inflammation in CRS (Frey *et al.,* 2013). As reported, IL-36γ drives neutrophil recruitment and corticosteroid resistance in CRS. Based on which, a novel mechanism of IL-36γ in tissue remodeling was revealed as follows: It upregulates the expression of MMP-9 by activating the p38 MAPK/ERK1/2 pathway, causing ECM degradation and basement membrane disruption. Hence, IL-36γexacerbates inflammation and directly promotes tissue remodeling by disrupting the mucosal barrier, establishing a vicious cycle. Therefore, targeting the IL-36γ-p38/ERK-MMP-9 axis may not only alleviate tissue damage but also indirectly suppress inflammation by restoring barrier integrity, offering a new therapeutic strategy for CRS. Under normal physiological conditions, the immune and physiological functions of nasal mucosa are in a balanced state. The symptom score in CRS group was markedly increased. The reason may be that the nasal mucosa of animals in CRS group had a strong inflammatory reaction during the sensitization and challenge process. Inflammation leads to nasal mucosal congestion, edema, increased mucus secretion, and impaired ciliary motility (Guan *et al.,* 2018), resulting in nasal congestion, rhinorrhea, and sneezing, which increase the nasal symptom score. The study found that the nasal symptom score in CRS group markedly surpassed control group, and nasal symptom scores in IL-36γ group and MAPK group were markedly lower versus CRS group, indicating that the IL-36γ and p38 MAPK/ERK1/2 pathways regulates pathological process of CRS.

Eosinophils are multifunctional white blood cells with immune regulatory functions. They maintain immune homeostasis in the body under baseline conditions and have autocrine and paracrine regulatory loops (Kita, 2011). Notably, our findings align with previous clinical observations that eosinophil infiltration is a hallmark of CRS and correlates with disease severity (Shin *et al.,* 2022). In CRS group, eosinophils, goblet cells and collagen fiber content in nasal mucosa tissue were increased compared with Control group; compared with CRS group, the number of eosinophils, goblet cells, and collagen fiber content in IL-36γ group were markedly reduced. IL-36γ acts in CRS remodeling (Shen *et al.,* 2023), while IL-36 is upregulated in inflammatory environments (Murrieta-Coxca *et al.,* 2019), binding to receptors on nasal mucosa cell and activate downstream pathways. If IL-36γ neutralizing antibody was adopted to inhibit its activity, the interaction between IL-36γ and its receptor was blocked. The chemotaxis and activation of eosinophils depend on inflammatory signals. After IL-36γ was inhibited, the expression of related chemokines decreased, and recruitment of eosinophils to nasal mucosa was reduced. Houtak *et al.* reported similarly that *Staphylococcus aureus* biofilm factors can induce goblet cell hyperplasia and mucosal damage in a rat rhinosinusitis model, further supporting the role of microbial factors in CRS (Houtak *et al.,* 2024). Inhibiting IL-36γ can reduce the stimulation of goblet cells, decrease their number, and alleviate the symptoms of excessive mucus secretion. For collagen fibers, inflammation promotes the activation of fibroblasts and collagen synthesis (Schuster *et al.,* 2021). Inhibiting IL-36γ reduces the level of inflammation, decreases the activation of fibroblasts, and thus reduces the content of collagen fibers. The neutralization of IL-36γ directly reduced its own level. Moreover, as an upstream signaling molecule, the reduction of IL-36γ affects the activation of downstream pathways. p38 MAPK regulates the activity of IL-4 and IL-5 promoter regulatory factors in T cells, as well as the Th2-specific transcription factor GATA-3 (Dodeller *et al.,* 2006). It can also upregulate IL-6, IL-8, and TNF-α (Li *et al.,* 2022). These regulatory functions are the basis of its obvious participation in the pathogenesis of AR, as confirmed by previous studies (Xiang *et al.,* 2022; Gao *et al.,* 2019). IL-36γ's inhibition reduces the phosphorylation of p38 and ERK, thereby suppressing transmission of pathways. Dai *et al.* reported that IL-1β regulates MMP-2 and MMP-9 via p38 pathway, impairing diabetic wound healing, showing a broad role of the p38/MMP-9 axis in tissue remodeling (Dai *et al.,* 2021). MMP-9 decreases as the pathway is suppressed. TNF-α and IL-6 production was significantly attenuated, demonstrating their dependence.

P38 MAPK pathway is the core of inflammatory response, which can regulate inflammation-related genes (Wang *et al.,* 2024). After activation, RAF kinase (MAPKKK) phosphorylates and activates elements in the MAPKK module MEK1/2 (Mao and Wang 2016). The inflammation-related gene expression decreases as the p38 MAPK/ERK1/2 pathway is suppressed, and IL-1β, p-p38, and MMP-9 protein levels are substantially reduced. Pathway inhibitors inhibit phosphorylation of p38 MAPK, thus blocking signal transmission. Li *et al.* found that IL-19 upregulates MMP-9 in human nasal epithelial cells via ERK/NF-κB signaling, which is consistent with ERK activation and MMP-9 up-regulation observed in CRS model (Li *et al.,* 2021). MMP-9 expression level is also regulated by this pathway, and its expression level is also reduced. Therefore, IL-36γ and p38 MAPK/ERK1/2 pathways have synergistic effects in the pathological process of CRS. IL-36γ upregulates the MMP-9 expression level by activating p38 MAPK/ERK1/2 pathway, causing destruction of nasal mucosa basement membrane and aggravation of inflammatory reaction. P38 MAPK/ERK1/2 pathway further aggravates the pathological state of nasal mucosa via regulations of eosinophil infiltration, goblet cells proliferation, and collagen fiber deposition.

Although this research has produced meaningful mechanical insights, there are still some limitations. Firstly, only male rats are used, and the interference of estrogen cycle is avoided, which excludes the potential gender difference in evaluating IL-36γ signal transduction in CRS, and the sample size is very small. It is worth noting that sexual dimorphism in immune response is recognized. Secondly, although the model induced by ovalbumin +LPS+SEB replicates the key features of human CRS, it does not fully capture the high heterogeneity of the disease, especially in distinguishing eosinophils from neutrophils. In addition, although the p38 MAPK inhibitor SB203580 is a classic pharmacological tool, the potential off-target effect can't be completely ruled out even though it contains a negative solvent control. Finally, the clinical relevance of these findings needs to be further verified in the population. It is worth noting that a recent groundbreaking study reported that IL-36γ in nasal mucosa of CRS patients was significantly up-regulated, especially those with fibrosis and high recurrence rate, and correlated it with epithelial-mesenchymal transition markers, which provided clinical support for our animal experimental results. In short, this study confirmed that IL-36γ considerably destroyed the nasal mucosa of CRS rats by activating p38 MAPK/ERK1/2 pathway, indicating that IL-36γ is the key link between inflammation and tissue remodeling. In the future, we should expand the sample size, including human studies, further clarify the underlying mechanism by using multi-omics technology, explore the treatment strategies and long-term safety of IL-36γ or p38 MAPK/ERK1/2 pathway, and provide more effective treatment options for CRS.

Conclusion: Utilizing the CRS rat model, this study found that the IL-36γ-mediated p38 MAPK/ERK1/2 pathway acts crucially in CRS pathological progression. By activating the p38 MAPK/ERK1/2 pathway, IL-36γ upregulates the expression of MMP-9, thereby inducing significant pathological alterations in the nasal mucosa. The findings suggest that targeting the inhibition of IL-36γ and related pathways may offer new therapeutic strategies for improving nasal mucosa integrity and inflammatory symptoms in CRS. This study elucidates novel mechanistic aspects of CRS pathogenesis and lays the foundation for developing therapeutic strategies targeting the IL-36γ/p38 MAPK/ERK1/2 pathway.

Authors' Contributions: Jia Zeng and Xiangsheng Li designed experiments; Jia Zeng and Xuejiao Li analyzed data; Jia Zeng and Xuejiao Li collected samples; Jia Zeng, Xuejiao Li and Xiangsheng Li performed experiments; Jia Zeng and Xiangsheng Li wrote the manuscript. All authors agreed to publish this article.

Funding: This work was supported by Research Project of Hunan Provincial Health Commission (D202307017000).

Animal rights statement: All animal experiments were approved by the Animal Ethics Committee of The Fourth Hospital of Changsha (Changsha, China), in compliance with Chinese national guidelines for the care and use of animals.

Conflict of interests: None

REFERENCES

Brzost, J., K. Czerwaty, K. Dżaman, N. Ludwig, K. Piszczatowska, and M.J. Szczepański (2022). Perspectives in Therapy of Chronic Rhinosinusitis. Diagnostics (Basel). 12(10): 2301. https://doi.org/10.3390/diagnostics12102301

Chen, J., J. Du, Y. Han, and Z. Wei (2021). Correlation analysis between IL-35, IL-36γ, CCL27 and psoriasis vulgaris. J Dermatolog Treat. 32(6): 621-624. https://doi.org/10.1080/09546634.2019.1689226

Chen, H., L. Tao, J. Liang, C. Pan, and H. Wei (2023). Ubiquitin D promotes the progression of rheumatoid arthritis via activation of the p38 MAPK pathway. Mol Med Rep. 27(2): 53. https://doi.org/10.3892/mmr.2023.12940

Cloitre, A., B. Halgand, S. Sourice, J. Caillon, O. Huck, I.M. Bugueno, F. Batool, J. Guicheux, V. Geoffroy, and P. Lesclous (2019). IL-36γ is a pivotal inflammatory player in periodontitis-associated bone loss. Sci Rep. 9(1): 19257. https://doi.org/10.1038/s41598-019-55595-9

Dai, J., J. Shen, Y. Chai, and H. Chen (2021). IL-1β Impaired Diabetic Wound Healing by Regulating MMP-2 and MMP-9 through the p38 Pathway. Mediators Inflamm. 2021: 6645766. https://doi.org/10.1155/2021/6645766

Dodeller, F., and H. Schulze-Koops (2006). The p38 mitogen-activated protein kinase signaling cascade in CD4 T cells. Arthritis Res Ther. 8(2): 205. https://doi.org/10.1186/ar1905

Emelyanova, A., A. Modestov, A. Buzdin, and E. Poddubskaya (2025). Role of ERK1/2 and p38 Protein Kinases in Tumors: Biological Insights and Clinical Implications. Front Biosci (Landmark Ed). 30(5): 31317. https://doi.org/10.31083/FBL31317.

Enache, I., E. IoniȚĂ, M. Mitroi, F. Anghelina, C. MogoantĂ, S. Ciolofan, A. CĂpitĂnescu, A. Stepan, and C. Simionescu (2020). Histopathological Features of Chronic Rhinosinusitis with Nasal Allergic Polyps. Curr Health Sci J. 46(1): 66-71. https://doi.org/10.12865/CHSJ.46.01.09

Frey, S., A. Derer, M.E. Messbacher, D.L. Baeten, S. Bugatti, C. Montecucco, G. Schett, and A.J. Hueber (2013). The novel cytokine interleukin-36α is expressed in psoriatic and rheumatoid arthritis synovium. Ann Rheum Dis. 72(9): 1569-1574. https://doi.org/10.1136/annrheumdis-2012-202264

Gabay, C., and J.E. Towne (2015). Regulation and function of interleukin-36 cytokines in homeostasis and pathological conditions. J Leukoc Biol. 97(4): 645-652. https://doi.org/10.1189/jlb.3RI1014-495R

Gao, X., N. Li, and J. Zhang (2019). SB203580, a p38MAPK inhibitor, attenuates olfactory dysfunction by inhibiting OSN apoptosis in AR mice (activation and involvement of the p38 mitogen-activated protein kinase in olfactory sensory neuronal apoptosis of OVA-induced allergic rhinitis). Brain Behav. 9(6): e01295. https://doi.org/10.1002/brb3.1295

Garlanda, C., C.A. Dinarello, and A. Mantovani (2013). The interleukin-1 family: back to the future. Immunity. 39(6): 1003-1018. https://doi.org/10.1016/j.immuni.2013.11.010

Guan, W.J., Y. Peng, X.X. Zi, K.S. Tan, T.T. He, N.S. Zhong, and Y. Wang (2018). Motile Ciliary Disorders in Chronic Airway Inflammatory Diseases: Critical Target for Interventions. Curr Allergy Asthma Rep. 18(9): 48. https://doi.org/10.1007/s11882-018-0802-x

Houtak, G., R. Nepal, G. Bouras, G. Shaghayegh, C. Bennett, J. Finnie, K. Fenix, A.J. Psaltis, P.J. Wormald, and S. Vreugde (2024). Staphylococcus aureus Biofilm-Secreted Factors Cause Mucosal Damage, Mast Cell Infiltration, and Goblet Cell Hyperplasia in a Rat Rhinosinusitis Model. Int J Mol Sci. 25(6): 3402. https://doi.org/10.3390/ijms25063402

Huang, Y., B. Yan, C. Meng, L. Zhang, and C. Wang (2024). Matrix metalloproteinases in chronic rhinosinusitis. Expert Rev Clin Immunol. 20(5): 547-558. https://doi.org/10.1080/1744666X.2024.2302362

Johnston, A., X. Xing, L. Wolterink, D.H. Barnes, Z. Yin, L. Reingold, J.M. Kahlenberg, P.W. Harms, and J.E. Gudjonsson (2017). IL-1 and IL-36 are dominant cytokines in generalized pustular psoriasis. J Allergy Clin Immunol IL-1 and IL-36 are dominant cytokines in generalized pustular psoriasis. J Allergy Clin Immunol. 140(1): 109-120. https://doi.org/10.1016/j.jaci.2016.08.056

Kim, D.W., K.M. Eun, H.R. Jin, S.H. Cho, and D.K. Kim (2016). Prolonged allergen exposure is associated with increased thymic stromal lymphopoietin expression and Th2-skewing in mouse models of chronic rhinosinusitis. Laryngoscope. 126(8): E265-E272. https://doi.org/10.1002/lary.26004

Kim, S.Y., M. Tang, S.Y. Chih, J. Sallavanti, Y. Gao, Z. Qiu, H.G. Wang, and W. Li (2025). Involvement of p38 MAPK and MAPKAPK2 in promoting cell death and the inflammatory response to ischemic stress associated with necrotic glioblastoma. Cell Death Dis. 16(1): 12. https://doi.org/10.1038/s41419-025-07335-3

Kita, H. (2011). Eosinophils: multifaceted biological properties and roles in health and disease. Immunol Rev. 242(1): 161-177. https://doi.org/10.1111/j.1600-065X.2011.01026.x

Kucuksezer, U.C., C. Ozdemir, M. Akdis, and C.A. Akdis (2018). Chronic rhinosinusitis: pathogenesis, therapy options, and more. Expert Opin Pharmacother. 19(16): 1805-1815. https://doi.org/10.1080/14656566.2018.1527904

Li, G., L. Duan, F. Yang, L. Yang, Y. Deng, Y. Yu, Y. Xu, and Y. Zhang (2022). Curcumin suppress inflammatory response in traumatic brain injury via p38/MAPK signaling pathway. Phytother Res. 36(3): 1326-1337. https://doi.org/10.1002/ptr.7391

Li, X., J. Huang, X. Chen, X. Lai, Z. Huang, Y. Li, S. Li, L. Chang, and G. Zhang (2021). IL-19 induced by IL-13/IL-17A in the nasal epithelium of patients with chronic rhinosinusitis upregulates MMP-9 expression via ERK/NF-κB signaling pathway. Clin Transl Allergy. 11(1): e12003. https://doi.org/10.1002/clt2.12003

Mao, L.M., and J.Q. Wang (2016). Synaptically Localized Mitogen-Activated Protein Kinases: Local Substrates and Regulation. Mol Neurobiol. 53(9): 6309-6315. https://doi.org/10.1007/s12035-015-9535-1

Murrieta-Coxca, J.M., S. Rodríguez-Martínez, M.E. Cancino-Diaz, U.R. Markert, R.R. Favaro, and D.M. Morales-Prieto (2019). IL-36 Cytokines: Regulators of Inflammatory Responses and Their Emerging Role in Immunology of Reproduction. Int J Mol Sci. 20(7): 1649. https://doi.org/10.3390/ijms20071649

Qiao, X.R., T. Feng, D. Zhang, L.L. Zhi, J.T. Zhang, X.F. Liu, Y. Pan, J.W. Xu, W.J. Cui, and L. Dong (2023). Luteolin alleviated neutrophilic asthma by inhibiting IL-36γ secretion-mediated MAPK pathways. Pharm Biol. 61(1): 165-176. https://doi.org/10.1080/13880209.2022.2160770

Schuster, R., J.S. Rockel, M. Kapoor, and B. Hinz (2021). The inflammatory speech of fibroblasts. Immunol Rev. 302(1): 126-146. https://doi.org/10.1111/imr.12971

Sedaghat, A.R., E.C. Kuan, and G.K. Scadding (2022). Epidemiology of Chronic Rhinosinusitis: Prevalence and Risk Factors. J Allergy Clin Immunol Pract. 10(6): 1395-1403. https://doi.org/10.1016/j.jaip.2022.01.016

Shen, L.F., H.H. Chen, and Y. Guo (2023). The role of interleukin 36γ in the epithelial-mesenchymal transition process of chronic rhinosinusitis: A pilot study. Clin Otolaryngol. 48(2): 347-355. https://doi.org/10.1111/coa.13993

Shin, S.H., M.K. Ye, J. Park, and S.Y. Geum (2022). Immunopathologic Role of Eosinophils in Eosinophilic Chronic Rhinosinusitis. Int J Mol Sci. 23(21): 13313. https://doi.org/10.3390/ijms232113313.

Tu, W., X. Chen, Q. Wu, X. Ying, R. He, X. Lou, G. Yang, K. Zhou, and S. Jiang (2020). Acupoint application inhibits nerve growth factor and attenuates allergic inflammation in allergic rhinitis model rats. J Inflamm. 17: 4. https://doi.org/10.1186/s12950-020-0236-9

Vlaminck, S., F. Acke, G.K. Scadding, B.N. Lambrecht, and P. Gevaert. (2021) Pathophysiological and Clinical Aspects of Chronic Rhinosinusitis: Current Concepts Front Allergy. 2: 741788. https://doi.org/10.3389/falgy.2021.741788

Wang, R., J. Liang, Q. Wang, Y. Zhang, Y. Lu, X. Zhan, S. Wang, and Q. Gu (2024). m6A mRNA methylation-mediated MAPK signaling modulates the nasal mucosa inflammatory response in allergic rhinitis. Front Immunol. 15: 1344995. https://doi.org/10.3389/fimmu.2024.1344995

Wißbrock, A., N.B. Goradia, A. Kumar, A.A. Paul George, T. Kühl, P. Bellstedt, R. Ramachandran, P. Hoffmann, K. Galler, J. Popp, U. Neugebauer, K. Hampel, B. Zimmermann, S. Adam, M. Wiendl, G. Krönke, I. Hamza, S.H. Heinemann, S. Frey, A.J. Hueber, O. Ohlenschläger, and D. Imhof (2019). Structural insights into heme binding to IL-36α proinflammatory cytokine. Sci Rep. 9(1): 16893. https://doi.org/10.1038/s41598-019-53231-0

Xiang, J., Z. Yang, and Q. Zhou (2022). Lidocaine relieves murine allergic rhinitis by regulating the NF-κB and p38 MAPK pathways. Exp Ther Med. 23(3): 193. https://doi.org/10.3892/etm.2022.11116